Appl. Phys. A 81, 1527–1531 (2005)
DOI: 10.1007/s00339-005-3390-2

Applied Physics A
Materials Science & Processing

F. SATO[1]
A.S. MOREIRA[2]
P.Z. COURA[3]
S.O. DANTAS[3,✉]
S.B. LEGOAS[5]
D. UGARTE[1,4]
D.S. GALVÃO[1]

Computer simulations of gold nanowire formation: the role of outlayer atoms

[1] Instituto de Física Gleb Wataghin, Universidade Estadual de Campinas, 13083-970 Campinas SP, Brazil
[2] Centro Brasileiro de Pesquisa Físicas, Rua Xavier Sigaud 150, 22290-180 Rio de Janeiro RJ, Brazil
[3] Departamento de Física, Universidade Federal de Juiz de Fora, 36036-900 Juiz de Fora MG, Brazil
[4] Laboratório Nacional de Luz Sincrotron, 13084-971 Campinas SP, Brazil
[5] Departamento de Fíisica, Universidade Federal do Amazonas, 66077-000 Manaus AM, Brazil

Received: 22 April 2005/Accepted: 23 August 2005
Published online: 5 October 2005 •

ABSTRACT Metallic nanowires (NWs) have been the object of intense theoretical and experimental investigations in the last years. In this work we present and review a new methodology we developed to study NW formation from mechanical stretching. This methodology is based on tight-binding molecular dynamics techniques using second-moment approximations. This methodology had been proven to be very effective in the study of NWs, reliably reproducing the main experimentally observed structural features. We have also investigated the problem of determining from what regions the atoms composing the linear atomic chains come. Our results show that ∼ 90% of these atoms come from outmost external layers.

PACS 66.30.Pa; 68.65.-k; 68.03.Hj

1 Introduction

In the last years a considerable effort has been devoted to understand the electronic and transport properties, as well as structural dynamics aspects, of metallic nanowires (NWs) and linear atomic suspended chains (LACs) [1–8]. The interest in these systems can be explained in part due to the observation of new phenomena at nanoscale (spin filters, quantized conductance [9, 10], etc.), and also to the new potential technological applications (molecular electronics, nanobiotechnology, nanocontacts, etc.).

Many theoretical studies have been carried out to investigate the electronic and structural behavior of metallic nanowires using different approaches: atomistic [2, 11–13], continuous [14, 15], or mixed model simulations applying empirical potentials [16–18], or even first-principles quantum-mechanical calculations [19–22]. Despite the amount of theoretical work carried out on these systems and the consequent and important gained knowledge, some fundamental aspects of the mechanism of formation and structural stability of NWs and LACs remain unclear, and there is a need for further studies. Among the limitations of some present theoretical methodologies, we can mention high computational cost, unrealistic pulling velocity, artificial periodic boundary conditions, and difficulties in incorporating the experimentally observed fact that different crystallographic orientations produce distinct results [8, 23]. Moreover, no systematic analysis for different crystallographic orientations has been carried out for these systems that takes into account the statistical aspects of the experimental conditions (sample-temperature fluctuations, grain size, boundaries, morphology, etc.).

In this work, we report theoretical studies of the elongation of gold NWs; mechanisms leading to the formation of LACs; the importance of contamination on experimental observations; and using the calculations to address the NW dynamic evolution.

✉ Fax: +55-32-3229-33-12, E-mail: dantas@fisica.ufjt.br

2 Methodology

In order to theoretically address the complex problem of NW formation, a realistic description that could incorporate the main experimental features, such as the different crystallographic orientations, is needed. In principle, structures with hundreds or thousands of atoms are necessary, which impose limitations on the methodologies to be used. The use of sophisticated ab initio methods is not possible but feasible with the use of simpler methods. Especially when we are mainly concerned with aspects such as structural features, the use of quantum methods is not mandatory and there are several non-quantum methods available that can handle very large systems.

2.1 *Parameter space*

In that sense we have developed a new computer code to address NW formation. It is based on tight-binding molecular dynamics (TB-MD) [24] techniques using second-moment approximations (SMA) [25] with a small set of adjustable parameters. This approximation is based on the well-known fact that cohesive properties of transition metals and their alloys are mainly dominated by the large *d*-band density of states (DOS). Besides that, structural quantities and metal thermodynamics are insensitive to the DOS details [26]; these magnitudes are dominated by the electronic bandwidth, associated with the second moment, and by the DOS average value, associated with the first moment. In this methodology the electronic structure arrangement near each atom is associated with the lattice topology. Thus, it is natural to describe the DOS in terms of moments, since moments are derived from

calculating products of matrix elements of the electron Hamiltonian along Brillouin-zone directions.

The cohesive energy E_c of the system can be obtained by

$$E_c = \sum_i \left[\sum_j A_{\alpha\beta} e^{-p_{\alpha\beta}\left(r_{ij}/r_0^{\alpha\beta}-1\right)} - \left[\sum_j B_{\alpha\beta}^2 e^{-2q_{\alpha\beta}\left(r_{ij}/r_0^{\alpha\beta}-1\right)} \right]^{1/2} \right], \quad (1)$$

where:

- $r_0^{\alpha\beta}$ represents the first-neighbor distance in a perfect crystalline $\alpha\beta$ lattice ($\alpha = \beta$ for pure metals and $\alpha \neq \beta$ for alloys);
- $r_{ij} = | \boldsymbol{r}_j - \boldsymbol{r}_i |$ is the distance between atoms i and j;
- $A_{\alpha\beta}$ represents the atom–atom repulsion;
- $p_{\alpha\beta}$ describes this repulsion dependence on the relative interatomic distance and is related to the system compressibility;
- $B_{\alpha\beta}$ represents an effective hopping integral;
- $q_{\alpha\beta}$ describes the dependence of the effective hopping integral on the relative interatomic distance.

The first contribution in Eq. (1) is associated with Born–Mayer repulsion type interaction; the second term (band contribution) ensures the system stability and is an attractive interaction with quantum-mechanical origin and many-body summations.

The parameters $A_{\alpha\beta}$, $B_{\alpha\beta}$, $p_{\alpha\beta}$, and $q_{\alpha\beta}$ can be obtained through a symplectic algorithm using experimental values for cohesive energy, lattice parameters (used to obtain $r_0^{\alpha\beta}$), and independent elastic constants for pure and alloy systems. The summation over j in Eq. (1) is crucial and depends on the kind of structure we are interested in; in general [24] up to fifth neighbors is enough to obtain a good description of cubic structures.

The symplectic algorithm makes use of the force equilibrium condition:

$$\boldsymbol{F}_j = \sum_{i \neq j} \boldsymbol{F}_{ij} = -\sum_{i \neq j} \nabla_i E_c = 0\,, \quad (2)$$

and the elastic constants at equilibrium are given by a theoretical development similar to that used in Ref. [27]. Indeed, we have a four-dimensional space in which to vary the parameters $A_{\alpha\beta}$, $B_{\alpha\beta}$, $p_{\alpha\beta}$, and $q_{\alpha\beta}$, in the sense that the equilibrium condition and the three independent elastic constants C_{11}, C_{12}, and C_{44} (Voigt notation for cubic crystals) are satisfied. This algorithm searches for a better set of parameters until the rms (root mean square) errors between the theoretical and experimental values for cohesive energy, lattice parameter, and elastic constants are less than 10^{-3} for each one of these properties.

As a test case we compared the parameters obtained with the use of this symplectic algorithm and those used in Refs. [24, 28] for bulk gold (Au). The experimental values for these parameters and the experimental conditions where they were obtained were taken from Refs. [29, 30].

The parameter sets are very similar with errors within 0.1 meV for $A_{\alpha\beta}$ and $B_{\alpha\beta}$, and 10^{-3} for $p_{\alpha\beta}$ and $q_{\alpha\beta}$. Our parameters are $A_{\mathrm{Au-Au}} = 0.2061$ eV, $B_{\mathrm{Au-Au}} = 1.790$ eV, $p_{\mathrm{Au-Au}} = 10.229$, and $q_{\mathrm{Au-Au}} = 4.036$ with lattice parameter $a = 4.0786$ Å.

In those situations where experimental information of cohesive energy, independent elastic constants, or even lattice parameters are not known, for instance in unusual metallic alloys, a first-principles quantum-mechanical calculation (density functional theory (DFT) or other approach) can be used to fulfill the needs.

2.2 *Dynamics simulations*

Once the cohesive energy (Eq. (1) and parameters) for Au is available, we can perform molecular dynamics simulations on all sorts of problems ranging from bulk systems (three-dimensional (3D) periodicity), surfaces (two-dimensional (2D) periodicity), slabs, clusters and – our main interest – NWs. As usual in molecular dynamics simulations, the linear momentum of the system must be conserved for all kinds of problems studied, and in the case of clusters special attention should be paid since our potential interaction includes many-body contributions (in the attractive term), so the angular momentum also should be conserved. The reason is that with this kind of many-body interaction and no periodicity a spurious torque can arise.

The temperature of the system is kept constant during each simulation using a rescaling velocity scheme [31]. The range of temperature that is possible to simulate can vary from 0 K) up to the melting point of the simulated structure, which depends on the number of particles in the system. Therefore, for each simulated system we have to determine this limiting temperature value. We have used pair correlation functions and heat-capacity values to monitor the phase transition from solid to liquid states. We used Beeman's algorithm [31] to integrate the equations of motion, with a time step of 2×10^{-15} s for all simulations. As we are interested in addressing the NW dynamical evolution, our methodology does not use (in contrast with most of the previous work reported in the literature) periodic boundary conditions. This allows a more effective way to contrast theoretical and the available experimental data. The use of TB-SMA potentials makes our code exceptionally fast, requiring typically only 1–2 h in a good Pentium IV for systems containing 500 atoms. The physical stress that generates the NWs is simulated through structural change dimensions (increasing the distance between the outmost NW layers, for instance); we have considered different elongation-rate variations.

To simulate the statistical aspects of experimental conditions, we used a random generator for the initial velocity distributions. Due to our low-cost computational simulations, we can generate many configurations to produce reliable statistical results of geometrical and other dynamical aspects, for example associated with crystallographic orientations, different apex crystallography, etc. In this way, the obtained results can be directly compared with the experimental data. Also, we can apply external torsion in a controllable way to mimic internal stress. This makes the present methodology a very effective tool in the study of metallic NWs generated by mechanical elongation.

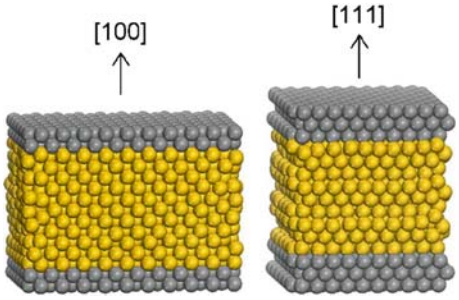

FIGURE 1 NW/apex epitaxial initial configurations. Two ([100] and [110]) or three ([111]) frontier layers are kept frozen during the simulations as buffer layers. The typical number of gold atoms in these systems is 1800

The atomistic initial geometric configurations are generated as a regular lattice for each crystallographic direction. In order to mimic the influence of the apex crystal orientation on the NW stability and dynamical growth, the frontier (initial and end wires) layers (two for [100] and [110], and three for [111]) are kept geometrically constrained during the simulations, which is sufficient for the NWs/apexes to preserve their epitaxial orientations (Fig. 1). These layers are free to move only along the NW elongation direction, but there are no other constraints for the remaining layers. The temperature of the system is kept constant until the system attains total energy equilibration; then we start to pull the wire along the NW growth direction. In our simulations we have considered temperatures varying from 300 up to 400 K, with typical elongation rates from 1 up to 5 m/s, and initial particle velocities randomly generated for each temperature value. All the atoms in the system contribute to the cohesive and kinetic energy.

During the molecular dynamics simulations detailed physical information can be obtained:

- for each gold atom we can monitor its motion (diffusion) and mean forces acting on it;
- on the apex: its morphological time evolution;
- on the whole system: its temperature, cohesive and kinetic energy, pair correlation function, energy fluctuation, heat capacity, etc.

3 Theory and experiment interplay

As mentioned before, from the experimental point of view, two techniques have been mostly used to produce nanowires: (a) in situ high resolution transmission electron microscopy (HRTEM) using methods developed by Takayanagi's [5, 32, 33] and other groups [8, 34, 35]; (b) mechanically controllable break junctions [3, 8, 36]. The former allows real-time visualization, providing a better evaluation of the dynamical atomistic aspects of NW elongation, while the latter in more appropriate for conductance experiments.

Molecular dynamics simulations can be used as an important tool to address some fundamental issues that are not directly accessible to experimental techniques.

For instance, in the break-junction experiments it is not possible to directly determine the specific morphological configurations associated with a specific conductance value while the NW is being formed. On the other hand, HRTEM experiments allow real-time visualization, but again the visualized structures cannot be directly associated with specific conductance peaks. Also, due to intrinsic two-dimensional (2D) aspects of the HRTEM acquired images, sometimes it is difficult to have a clear idea of the three-dimensional aspects from 2D images. In this sense molecular dynamics simulations can provide helpful information to the experimentalists, not only accessing time-scale phenomena inaccessible from the experiments, but also helping to test 3D models built from 2D data information.

In Sect. 4 we will discuss some of these points and present results from molecular dynamics simulations. One important issue here is whether parameters obtained from the bulk gold system can reproduce experimental behavior at the nanoscale. The answer to this question is associated with our comprehension that the main contribution to the dynamic morphologies of metal nanowires, in the temperature range studied, comes from the kinetics of the system. Thus, the parameters from the bulk can be used for NW studies.

The reliability of our method was tested for di-, tri-, and tetramer energy profiles versus the interatomic distances. As we can see from Fig. 2, the qualitative features of the curves are very similar to the ones from DFT calculations [21]. The predicted equilibrium distances (2.46 Å for the tetramer) compare well with DFT results (2.44–2.49 Å) [21] and experimental data (2.47 Å) [37].

Also, the repulsive part of the interaction energy for the dimer is softer in SMA than in DFT. When many-body summations take place the repulsive part of the interaction energy (in the trimer and tetramer) becomes harder. Therefore, the explicit electronic contribution, for the dimer, should block shorter Au−Au distances and increase a little its equilibrium distance by 5–7%. On the other hand, the tension imposed on the NWs should favor longer Au−Au distances [5, 6, 8, 33, 34], but in some situations this range of interatomic distances can only be explained by carbon (C) contamination [21].

Considering systems containing typically 500 atoms, computer simulation time depends on the pulling velocity, but a typical run takes $\sim$ 160 ps to equilibrate the system at a specific temperature of 300–400 K. After thermalization we start

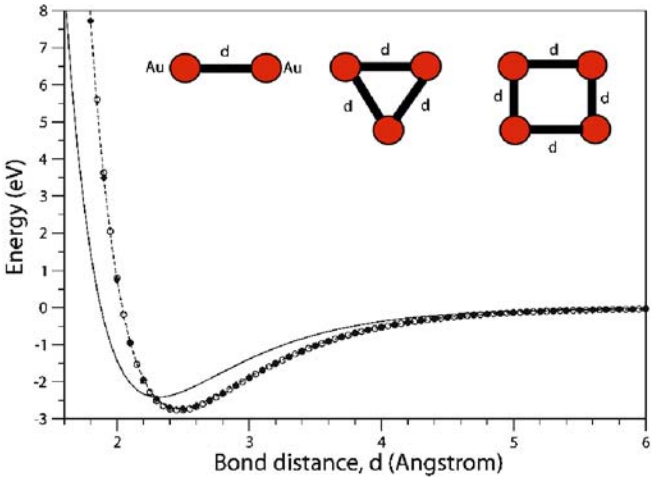

FIGURE 2 Au−Au SMA energy as a function of the interatomic distance for dimer (*black solid line*), trimer (*black dashed line with black filled diamond symbols*), and tetramer (*open black circle symbols*)

to pull the system along [100], [110], or [111] crystal directions with velocity in the range 1–5 m/s, which corresponds to a simulation of 240–40 ps, respectively. Therefore, the total simulation time is in the range 200–400 ps and we can follow the structural system behavior on a time scale that the HRTEM experiments could not observe since the images are acquired at 30 frames per second (fps).

4 Results and discussion

We have successfully used this methodology to study some structural features of the gold NW formation [38]. We have used the same methodologies for other fcc metals as Cu [39] and work for Pt, Al, Ag, Ni, and Pb is in progress.

Here we would like to address the important question: from which region do the atoms that compose the final stages of the suspended atom chains (LACs) come? This is a problem difficult to address from HRTEM experiments but properly feasible from molecular dynamics simulations.

We present in Fig. 3 snapshots from a computer simulation for a nanowire with 1680 ($10 \times 8 \times 21$) Au atoms; the stretching velocity was 3 m/s along the [110] direction (vertical direction), the system temperature was 350 K, and the total simulation time was 240 ps. We used different colors to 'mark' surface and bulk gold atoms. Grey balls represent surface atoms and yellow bulk ones. We then follow their time evolution as the NW is stretched until a LAC is formed. From Fig. 3 it is clear that mainly surface atoms compose the linear atomic chains (LACs). A better visual analysis can be made from the video (complementary material – movie 1).

Our statistical analysis for this behavior showed that typically 90% of the atoms composing the LACs come from the outmost external layers. This seems to be a general feature for other metals such as Cu and Ag [40].

This is an interesting result and can perhaps help to explain the important role played by carbon contaminants, as recently proposed [21, 41]. If in fact carbon atoms are present as contaminants in the LACs, it is more likely that they could be incorporated arising from the surface rather than from the bulk. Our results showing that this configuration is the most probable one adds support for this interpretation.

Another peculiar feature observed from the simulations is associated with the aspect ratio of the nanowire. In Fig. 4 we present snapshots from a simulation for a nanowire with 1800 ($12 \times 10 \times 15$) Au atoms; the pulling velocity was 3 m/s along the [111] direction (vertical direction), the system temperature was set to 350 K, and the total simulation time was 240 ps. From these snapshots we can see LACs formed from columnar formations with small clustering (on the left-hand column) just before junction breaking. Looking at the video (complementary material – movie 2) of this simulation, the left-hand column breaks first and the LAC evolves until breaking with five atoms in it.

These multicolumnar structures have not been observed in HRTEM experiments; they are unlikely to occur due to the aspect ratio of the crystal grains. These kinds of structures are more likely to occur in break-junction experiments. In fact, they have been predicted to occur by Correia and co-workers [42] and our results are consistent with their predictions and could help to explain some fluctuations in the conductance data. More investigations along these lines are needed.

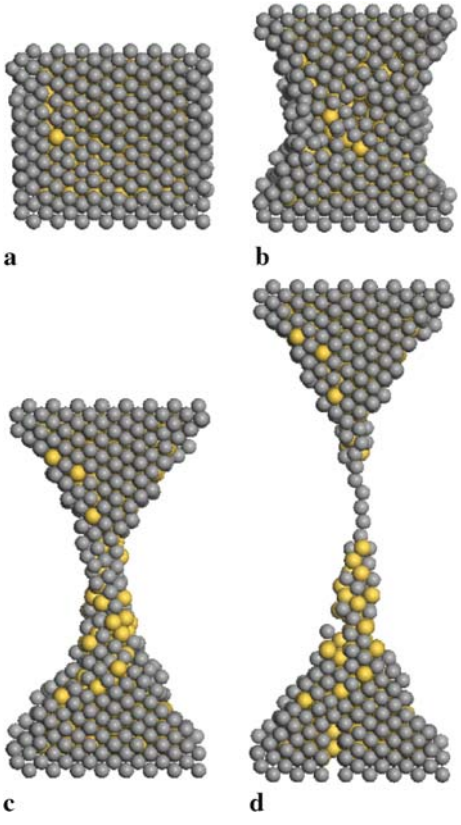

FIGURE 3 Snapshots of a computer simulation along the [110] direction with 1680 ($10 \times 8 \times 21$) Au atoms, *dark grey balls* represent surface atoms and *yellow balls* represent bulk atoms. We can see that mainly surface atoms form the LAC

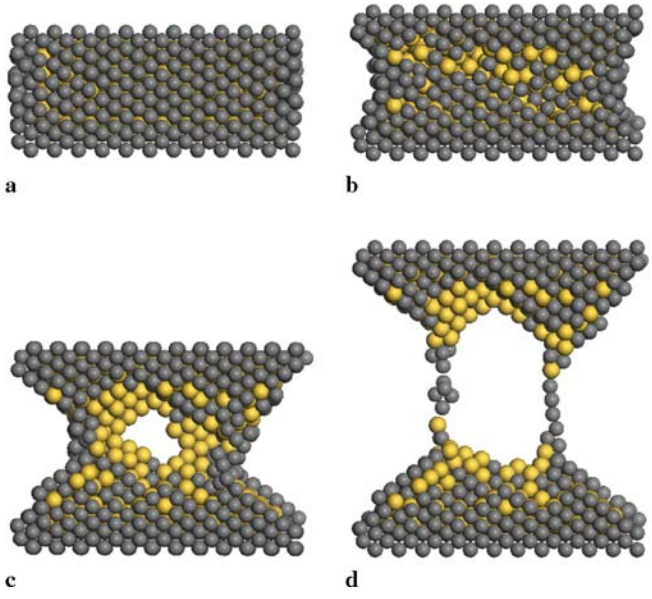

FIGURE 4 Snapshots of a computer simulation along the [111] direction with 1800 ($12 \times 10 \times 15$) Au atoms. *Dark grey balls* represent surface atoms and *yellow* bulk ones. We can see that mainly surface atoms form the LACs. In this case we see columnar ((**c**) and (**d**) snapshots) formation, an aspect-ratio issue that cannot appear in Fig. 3

ACKNOWLEDGEMENTS The authors acknowledge financial support from the Brazilian Agencies CAPES, CNPq, IMMP/MCT, IMN/MCT, FAPEMIG, and FAPESP.

REFERENCES

1 N. Agraït, A.L. Yeati, J.M. van Ruitenbeek, Phys. Rep. **377**, 81 (2003)
2 U. Landman, W.D. Luedtke, N.A. Burnham, R.J. Colton, Science **248**, 454 (1990)
3 J.M. Krans, J.M. van Ruitenbeek, V.V. Fisun, I.K. Yanson, L.J. de Jongh, Nature (Lond.) **375**, 767 (1995)
4 U. Landman, W.D. Luedtke, B.E. Salisbury, R.L. Whetten, Phys. Rev. Lett. **77**, 1362 (1996)
5 H. Ohnishi, Y. Kondo, K. Takayanagi, Nature **395**, 780 (1998)
6 A.I. Yanson, G. Rubio Bollinger, H.E. van den Brom, N. Agraït, J.M. van Ruitenbeek, Nature **395**, 783 (1998)
7 D. Sánchez-Portal, E. Artacho, J. Junquera, P. Ordejón, A. Garcia, J.M. Soler, Phys. Rev. Lett. **83**, 3884 (1999)
8 V. Rodrigues, T. Fuhrer, D. Ugarte, Phys. Rev. Lett. **85**, 4124 (2000)
9 E. Medina, A. Hamsy, P.A. Serena, Phys. Rev. Lett. **86**, 5574 (2001)
10 P. Garía-Mochales, S. Peláes, P.A. Serena, E. Medina, A. Hamsy, Appl. Phys. A (the present issue)
11 M.R. Sorensen, M. Brandbyge, W. Jacobsen, Phys. Rev. B **57**, 3283 (1998)
12 E.Z. da Silva, A.J.R. da Silva, A. Fazzio, Phys. Rev. Lett. **87**, 256 102 (2001)
13 J.W. Kang, H.J. Hwang, Nanotechnology **13**, 503 (2002)
14 C.A. Stafford, D. Baeriswyl, J. Bürki, Phys. Rev. Lett. **79**, 2863 (1997)
15 C. Yannouleas, U. Landman, J. Phys. Chem. B **101**, 5780 (1997)
16 N.D. Lang, Phys. Rev. Lett. **79**, 1357 (1997)
17 C.C. Wan, J.-L. Mozos, G. Taraschi, J. Wang, H. Go, Appl. Phys. Lett. **71**, 419 (1997)
18 L.G.C. Rego, A.R. Rocha, V. Rodrigues, D. Ugarte, Phys. Rev. B **67**, 045 412 (2003)
19 R.N. Barnet, U. Landman, Nature (Lond.) **87**, 788 (1997)
20 A. Nakamura, M. Brandbyge, L.B. Hansen, K.W. Jacobsen, Phys. Rev. Lett. **82**, 1538 (1999)
21 S.B. Legoas, D.S. Galvão, V. Rodrigues, D. Ugarte, Phys. Rev. Lett. **88**, 076 105 (2002)
22 D. Kruger, H. Fuchs, R. Rousseau, D. Marx, M. Parrinello, Phys. Rev. Lett. **89**, 186 402 (2002)
23 V. Rodrigues, J. Bettini, A.R. Rocha, L.G.C. Rego, D. Ugarte, Phys. Rev. B **65**, 153 402 (2002)
24 F. Cleri, V. Rosato, Phys. Rev. B **48**, 22 (1993)
25 D. Tomanek, A.A. Aligia, C.A. Balsero, Phys. Rev. B **32**, 5051 (1985)
26 F. Ducastelle, J. Phys. **31**, 1055 (1970)
27 M.S. Daw, M.I. Baskes, Phys. Rev. B **29**, 6443 (1984)
28 F. Cleri, G. Mazzone, V. Rosato, Phys. Rev. B **47**, 14 541 (1993)
29 C. Kittel, *Introduction to Solid State Physics* (Wiley, New York 1996)
30 G. Simmons, H. Wang, *Single Crystal Elastic Constants and Calculated Aggregated Properties* (MIT Press, Cambridge, MA 1971)
31 M.P. Allen, D.J. Tildesley, *Computer Simulation of Liquids* (Oxford University Press, Oxford 1996)
32 Y. Kondo, K. Takayanagi, Phys. Rev. Lett. **79**, 3455 (1997)
33 H. Koizumi, Y. Oshima, Y. Kondo, K. Takayanagi, Ultramicroscopy **88**, 17 (2001)
34 V. Rodrigues, D. Ugarte, Phys. Rev. B **64**, 073 405 (2001)
35 T. Kizuka, S. Umehaa, S. Fujosawa, Jpn. J. Appl. Phys. **240**, L71 (2001)
36 C.J. Muller, J.M. van Ruitembeek, L.J. de Jongh, Physica C **191**, 485 (1992)
37 O.D. Häberlen, S.C. Chung, N. Rösch, Int. J. Quantum Chem. **28**, 595 (1994)
38 P.Z. Coura, S.B. Legoas, A.S. Moreira, F. Sato, V. Rodrigues, S.O. Dantas, D. Ugarte, D.S. Galvão, Nano Lett. **47**, 1187 (2004)
39 J.C. González, V. Rodrigues, J. Bettini, L.G.C. Rego, P.Z. Coura, S.O. Dantas, F. Sato, D.S. Galvão, D. Ugarte, Phys. Rev. Lett. **93**, 126 103 (2004)
40 F. Sato et al., unpublished
41 S.B. Legoas, V. Rodrigues, D. Ugarte, D.S. Galvão, Phys. Rev. Lett. **93**, 216 103 (2004)
42 A. Correia, M. Marquéz, N. García, in *Nanowires*, ed. by P. Serena, N. García (NATO ASI Ser. E: Appl. Sci. **340**) (Kluwer, Dordrecht 1997) p. 311